

Available online at www.sciencedirect.com**ScienceDirect**journal homepage: <http://www.elsevier.com/locate/rpor>**Original research article****Feasibility study on the use of 230 MeV proton cyclotron in proton therapy centers as a spallation neutron source for BNCT****E. Nobakht*, N. Fouladi**

Department of Nuclear Physics, University of Tabriz, Tabriz 51664, Iran

ARTICLE INFO**Article history:**

Received 7 November 2018

Received in revised form

23 July 2019

Accepted 7 October 2019

Available online 30 October 2019

Keywords:

Beam Shaping Assembly (BSA)

Boron neutron capture therapy

(BNCT)

MCNPX2.6

Spallation neutron source

Proton accelerator

ABSTRACT

Aim: The feasibility of using 230 MeV proton cyclotrons in proton therapy centers as a spallation neutron source for Boron Neutron Capture Therapy (BNCT) was investigated.

Background: BNCT is based on the neutron irradiation of a ^{10}B -containing compound located selectively in tumor cells. Among various types of neutron generators, the spallation neutron source is a unique way to generate high-energy and high-flux neutrons.

Materials and Methods: Neutron beam was generated by a proton accelerator via spallation reactions and then the produced neutron beam was shaped to be appropriate for BNCT. The proposed Beam Shaping Assembly (BSA) consists of different moderators, a reflector, a collimator, as well as thermal and gamma filters. In addition, the simulated Snyder head phantom was utilized to evaluate the dose distribution in tumor and normal tissue due to the irradiation by the designed beam. MCNPX2.6 Monte Carlo code was used to optimize BSA as well as evaluate dose evaluation.

Results: A BSA was designed. With the BSA configuration and a beam current of 104 nA, epithermal neutron flux of 3.94×10^6 [n/cm²] can be achieved, which is very low. Provided that we use the beam current of 5.75 μA , epithermal neutron flux of 2.18×10^8 [n/cm²] can be obtained and the maximum dose of 38.2 Gy-eq can be delivered to tumor tissue at 1.4 cm from the phantom surface.

Conclusions: Results for 230 MeV protons show that with proposed BSA, proton beam current about 5.75 μA is required for this purpose.

© 2019 Greater Poland Cancer Centre. Published by Elsevier B.V. All rights reserved.

1. Introduction

Boron Neutron Capture Therapy (BNCT) is a binary cancer therapy modality which has attracted extensive interest in recent decades due to its potential for selective cell killing.¹

BNCT has led to many important therapeutic applications in diverse areas of cancer treatment with notable examples in brain, skin, lung, liver, prostate, head and neck tumors^{2–4} for which conventional therapies, like chemotherapy, surgery, and radiotherapy are not completely successful. The idea of BNCT dates back to 1936 when Locher initially recognized the

* Corresponding author.

E-mail address: nobakhtesmail@gmail.com (E. Nobakht).

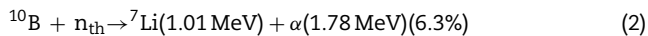
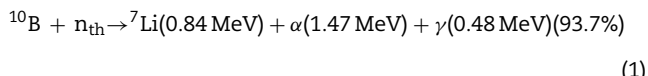
<https://doi.org/10.1016/j.rpor.2019.10.005>

1507-1367/© 2019 Greater Poland Cancer Centre. Published by Elsevier B.V. All rights reserved.

therapeutic potential of Boron Neutron Capture reaction, i.e. $^{10}\text{B}(\text{n},\alpha)^7\text{Li}$, which was four years after the discovery of neutron by Chadwick.⁵

BNCT has two key steps. In the first step, a boron-containing compound, such as Boron Phenylalanine (BPA) or Borocaptate Sodium (BSH), is administered to the patient such that they it is deposited on the tumor more than normal tissue. In the next step, tumor area is subjected to the neutron irradiation.⁶

During neutron irradiation, ^{10}B promptly disintegrates into two high linear-energy-transfer (LET) particles, an α particle and ^7Li nucleus, via the $^{10}\text{B}(\text{n},\alpha)^7\text{Li}$ reaction (1)-(2)^{7,8}:



The high-LET radiation released in the tumor cells by the interaction of ^{10}B with thermal neutrons would be sufficient to kill or sterilize the tumor cells; and the short-range ($<10 \mu\text{m} \sim \text{cell diameter}$) of the particles produced by the neutron capture reaction could limit the damage to the cells containing ^{10}B .

Most used neutron sources for BNCT are reactors, so the number of BNCT centers are limited. Since the accelerator-based BNCT (AB-BNCT) has much lower costs than the reactor-based BNCT (RB-BNCT), the AB-BNCT is being established worldwide as the future modality to start the era of in-hospital facilities. For this reason, the neutron production based on spallation reactions using accelerators in proton therapy centers was evaluated in this research. In order to provide an appropriate neutron beam, a Beam Shaping Assembly (BSA) should be designed based on the neutron source specifications. The aim of the present work is to perform a feasibility study on the use of 230 MeV proton cyclotron in proton therapy centers as neutron source for BNCT. For this purpose, the proton accelerator (104 nA)⁹ in Boston proton therapy center in the United States of America was considered. Simulations were performed by using the Monte Carlo code MCNPX2.6, with the Los Alamos LA150 data library ($E \leq 150 \text{ MeV}$) and physical models embedded in the code ($E \geq 150 \text{ MeV}$),¹⁰ for the design of the target and BSA and considering the dose distribution in the depth of the head phantom. In this study, neutrons having energies below 1 eV, between 1 eV and 10 keV and above 10 keV are referred to as thermal, epithermal and fast neutrons, respectively. Usually, cancer cells are located deeper inside the human body, and in these cases, it is generally accepted that epithermal neutron beams of energy $\sim 10 \text{ keV}$ are optimal.¹¹

2. Aim

This work aims to explore the application feasibility of 230 MeV proton cyclotrons in proton therapy centers to be used as a spallation neutron source for BNCT.

3. Materials and methods

3.1. Neutron and photon transport calculations

In this study, neutron and photon transport simulations from the neutron source to the head phantom were performed using Monte Carlo MCNPX2.6 code in order to optimize the spallation target, the BSA design and compute the dose distribution in a head phantom for a BNCT facility. Variance reduction techniques, such as geometry splitting with Russian roulette have been utilized to decrease the simulation time. The Los Alamos LA150 data library ($E \leq 150 \text{ MeV}$) and physical models embedded in the code ($E \geq 150 \text{ MeV}$) have been used in the simulations.

3.2. Spallation target

Generally, heavy nuclei are used for spallation targets because the neutron production in the spallation process is the most efficient for large nuclei.¹² Tantalum (Ta), Tungsten (W), Mercury (Hg), Lead (Pb), Lead-Bismuth eutectic (LBE) can be used as a target material, but the use of non-actinide materials, such as Ta, W, and Pb, became the unique solution suggested to be used as solid targets at beam power levels far below 1 MW and the liquid targets at higher power.¹² Neutron yield is one of the most significant factors in the selection of target material. Heat transfer characteristics and thermal resistance are the other important factors for choosing the target material.¹³ In this study, Ta, W, Pb, LBE and Bi were tested as spallation target materials and simulations for materials with different dimensions were performed to obtain the best material in optimum dimension as well as appropriate angle of spallation target relative to the proton beam direction. A comparison between the parameters used in this study and some existing spallation neutron sources are listed in Table 1.

3.3. Design and optimization of BSA

A BSA facility should be designed with the intention of moderating high-energy neutrons from the spallation reactions to lower energies as well as eliminate fast and thermal neutrons and gamma contaminations in order to satisfy the International Atomic Energy Agency (IAEA) recommendation (Table 2).¹¹ Every BSA facility consists of several layers of different materials, including reflector, moderator, collimator thermal neutron filter, and gamma filter.

The moderator should have a high fast neutron scattering cross-section ($\sum_{s,\text{fast} \rightarrow \text{epi}}$) and low epithermal neutron scattering and absorption cross-sections ($\sum_{r \rightarrow \text{epi}}$), so that the value of $\sum_{s,\text{fast} \rightarrow \text{epi}} / \sum_{r \rightarrow \text{epi}}$ parameter is as high as possible. Moreover, the moderator should have a low fast neutron absorption cross-section because fast neutrons will be removed from the spectrum and cannot contribute to the lower energy regions anymore. In addition, gamma contamination due to neutron interactions should be as low as possible in the BSA.⁷

A reflector decreases the neutron leakage and can further improve the quality of the beam.¹¹

Table 1 – Main parameters of some existing spallation neutron sources.

Accelerator	Proton kinetic energy	Beam current	Target material
SNS Oak Ridge ¹⁴	1.0 GeV	1.4 mA	Hg
KENS Japan ¹⁵	500 MeV	10 μA	W (Ta Clad)
LNSC Los Alamos ¹⁶	800 MeV	80 μA	W
ISIS Oxford ¹⁷	800 MeV	200 μA	W (Ta Clad)
SINQ Villigen ¹⁸	590 MeV	2.3 mA	Pb Rods (in Zircaloy Tubes)
IPNS Argonne USA ¹⁹	450 MeV	15 μA	U ²³⁸
Mass General Hospital, Boston, MA (which was evaluated in this study) ⁹	230 MeV	104 nA	W

Table 2 – Recommended values in the beam exit window¹¹ (Ø symbolizes the flux and D symbolizes the dose rate).

BNCT in-air parameters	Recommended value
Øepithermal [n/cm ² s]	~1 × 10 ⁹
Øepithermal/Øfast	>20
Øepithermal/Øthermal	>100
D _{fast} /Øepithermal [Gycm ² /n]	<2 × 10 ⁻¹³
D _γ /Øepithermal [Gycm ² /n]	<2 × 10 ⁻¹³
J/Ø ^a	>0.7
Fast energy group Ø _{fast}	E>10 keV
Epithermal energy group Ø _{epi}	1 eV ≤ E ≤ 10 keV
Thermal energy group Ø _{th}	E<1 eV

^a The ratio between the total neutron current and the total neutron flux.

The beam collimator should be designed in order to maximize the dose delivered to the tumor and minimize the dose delivered to the rest of the body. In fact, collimators can be used to improve the ratio of current to flux of the final incident beam.²⁰

As mentioned before, in order to obtain an epithermal neutron beam with high quality, the undesired gamma rays as well as thermal and fast neutrons are removed using appropriate filters. Several sets of materials have been considered and the neutron spectra have been investigated based on energy and intensity. In this study, materials including Iron (Fe), Aluminum (Al) and Magnesium Fluorine (MgF₂) were tested as the moderators. Iron has high inelastic scattering cross section above 860 keV, a window at 20 keV and it decreases the fast neutron flux below the 100 keV.²¹ Magnesium fluorine also presents a good performance in terms of neutrons accumulation inside the epithermal energy range; magnesium and fluorine have strong resonance structures in elastic scattering cross section for fast neutrons and also these two elements have relatively small mass numbers. Aluminum has a low enough first excited state to make useful inelastic scattering, and it is ideal to decrease the high neutron flux in the range of >843.8 keV. The size of the moderators was optimized by parametric studies from the perspective of the dose depth distribution, the absolute dose to tumor tissue and the therapeutic time.

Beam quality is evaluated by parameters recommended by IAEA for BNCT (Table 2).

Table 3 – The phantom materials and dimensions.⁶

Snyder head phantom	
Material	Water and Liquid-B
Geometry	Ellipsoidal
Diameter (cm)	16
Length (cm)	20
PMMA wall thickness (mm)	2

3.4. Dose evaluation

Absorbed dose delivered to the normal tissue and tumor during BNCT result from possible reactions. Four major dose components in BNCT are the dose from the ¹⁰B(n,α)⁷Li capture reaction, D_B; the dose due to ¹⁴N(n,p)¹⁴C reaction, D_N; the neutron dose from fast neutrons, D_F; and the γ ray dose from γ ray contamination in the neutron beam and neutron capture reaction, D_γ.²²

The weighted dose commonly known as total biologically weighted dose (D_T) for the patient is defined as a sum of four physical dose components each multiplied by a specific biological weighting factor according to Eq. (3)²⁰:

$$D_T = C_B \cdot w_B \cdot D_B + w_N \cdot D_N + w_F \cdot D_F + w_\gamma \cdot D_\gamma [\text{Gy-equivalent}] \quad (3)$$

C_B is the boron concentration in the tissue in units of ppm. Boron concentration in the tumor must be higher than boron concentration in the normal brain. The weighting factors w_N and w_F are taken as 3.2, and w_γ is considered to be 1.0 in the tumor and normal tissue. w_B is assumed to be 1.3 and 3.8 in the normal tissue and the tumor, respectively. Flux to dose conversion factors were utilized to calculate each dose component. The weighting factors were taken from values used in BNL's protocol.²³ The computational head phantom model is Snyder, which consists of the skin, the skull, the head volume and the tumor.

In this paper, the Snyder head phantom with anatomical structures (skin, skull, brain and possibly tumor) was utilized to test the important aspects of the treatment planning codes, such as dose volume calculation. The phantom material and dimensions are described in Tables 3 and 4.²⁴ The used head phantom ellipsoidal geometry is described in Eqs. (4)–(6).²⁵

$$(x/6)^2 + (y/9)^2 + ((z-1)/6.5)^2 = 1(\text{brain-skullboundary}) \quad (4)$$

$$(x/6.8)^2 + (y/9.8)^2 + (z/8.3)^2 = 1(\text{skull-skinboundary}) \quad (5)$$

$$(x/7.3)^2 + (y/10.3)^2 + (z/8.8)^2 = 1(\text{skull-airboundary}) \quad (6)$$

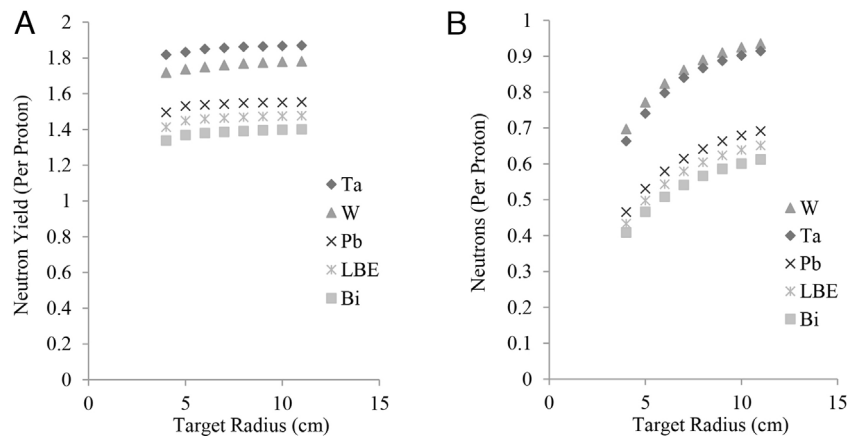


Fig. 1 – (A) Neutron yield of spallation targets in different radii. (B) Number of neutrons on the surface in different radii.

Table 4 – The Snyder phantom material, according to ICRU report 46 (ICRU 1992).

Element	Tissue		
	Brain	Skin	Cranium
Density (g/cm ³)	1.040	1.090	1.610
Hydrogen	10.7	10	5
Carbon	14.5	20.4	21.2
Nitrogen	2.2	4.2	4
Oxygen	71.2	64.5	43.5
Sodium	0.2	0.2	0.1
Phosphorus	0.4	0.1	8.1
Sulfur	0.2	0.2	0.3
Chlorine	0.3	0.3	–
Potassium	0.3	0.1	–
Calcium	–	–	17.6
Magnesium	–	–	0.2

4. Results and discussion

4.1. Optimal spallation target

As shown in Fig. 1, Ta and W have the highest neutron yield in the mentioned materials; So W was selected as the spallation target because of having a higher melting point.

To determine the optimal dimension of the target, thickness and radius of the cylindrical target were changed in the range of 1–6 cm and 2–14 cm, respectively. Then, the neutrons on the surface of the target were studied.

As expected, the number of produced neutrons in the dimension more than the proton range in the target (based on SRIM calculation, 3.27 cm for 230 MeV in W) is increased gradually. Simulation results from Fig. 2 indicate that increasing the radius causes nuclear spallation reactions and (n, nx) reactions by secondary particles themselves.¹² Therefore, the production of neutrons in the target will increase.

As seen in Fig. 2, no significant changes will occur in the number of neutrons in the dimensions greater than 7 cm in radius and 3 cm in thickness, so they were selected as the dimensions of the spallation target.

The next step is to determine an optimum angle of the target relative to the incident proton beam direction. In the

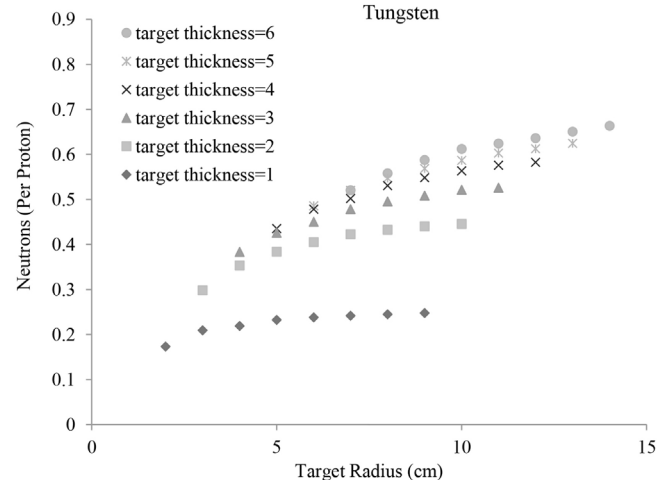


Fig. 2 – Number of neutrons on the surface of the W target for different radii.

optimum angle, most neutrons move close to the forward direction at small angles. Because neutrons that move at greater angles relative to the forward direction may change to thermal neutrons by multiple collisions. The optimum angle was calculated based on the simulation results of neutron spectra at the entrance of the BSA for various target angles. Therefore, the target was inclined 40 degrees relative to the proton beam direction. Calculated neutron spectra at the entrance of the BSA for four angles are given as samples in Fig. 3.

4.2. Beam Shaping Assembly design

Table 5 shows the calculated figures of merit (FOM) for various thicknesses of Iron moderator as an example. Iron with 15 cm thickness was selected due to its ability to decrease the fast neutron dose (Fig. 4) (D_{max} for both thicknesses are approximately equal).

In order to obtain a neutron beam suitable for BNCT, a thermal neutron filter is essential. Numerous simulations have been carried out and the results show that Lithium Fluoride

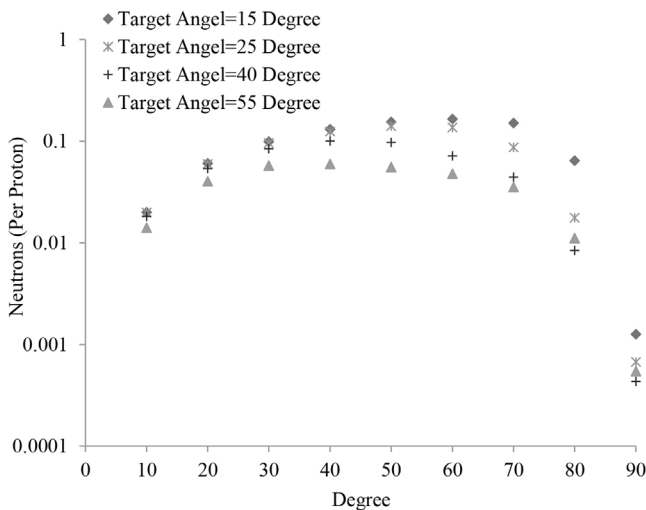


Fig. 3 – Calculated neutron spectra at the entrance of the BSA for various target angles relative to the proton beam direction.

Table 5 – In-air parameters for different thicknesses of iron moderator.

Neutron beam parameters	10 cm Fe	15 cm Fe	20 cm Fe
$\emptyset_{\text{epi}}/\emptyset_{\text{fast}}$	2.16E+1	2.73E+1	2.91E+1
$\emptyset_{\text{epi}}/\emptyset_{\text{th}}$	1.62E+2	1.38E+2	1.42E+2
$\emptyset_{\text{epi}} [\text{n/cm}^2\text{s}]$	4.59E+6	3.94E+6	3.31E+6
$\dot{D}_{\text{fast}}/\emptyset_{\text{epi}} [\text{Gycm}^2/\text{n}]$	9.16E-15	7.34E-15	8.87E-15
$\dot{D}_{\gamma}/\emptyset_{\text{epi}} [\text{Gycm}^2/\text{n}]$	3.64E-14	3.38E-14	3.09E-14

Table 6 – In-air parameters for different gamma shields.

Neutron beam parameters	Bi	Pb
$\emptyset_{\text{epi}}/\emptyset_{\text{fast}}$	2.73E+1	2.63E+1
$\emptyset_{\text{epi}}/\emptyset_{\text{th}}$	1.38E+2	1.28E+2
$\emptyset_{\text{epi}} [\text{n/cm}^2\text{s}]$	3.94E+6	3.94E+6
$\dot{D}_{\text{fast}}/\emptyset_{\text{epi}} [\text{Gycm}^2/\text{n}]$	7.34E-15	7.97E-15
$\dot{D}_{\gamma}/\emptyset_{\text{epi}} [\text{Gycm}^2/\text{n}]$	3.38E-14	3.35E-14
$J_{\text{epi}}/\emptyset_{\text{epi}}$	7.97E-1	7.94E-1

and Cadmium can improve the quality of the beam. Instead of utilizing a thick layer of Lithium Fluoride as a thermal neutron filter, Lithium Fluoride filters have been placed between different layers of moderator materials. By doing so, epithermal neutron flux increases and at the same time gamma rays produced by BSA components decrease, especially the gamma rays produced by Aluminum.

Gamma neutron contamination should be limited by filtering. Lead (Pb) and Bismuth (Bi) are used as gamma ray filters. Both materials were tested and, even though Lead is an excellent gamma ray filter, it increases both thermal neutron dose and fast neutron dose (Fig. 5 and Table 6). As seen in Figs. 5 and 6, total delivered dose to tumor and gamma dose using both filters are the same. Therefore, 0.5 cm of Bismuth in optimized thickness was used as a gamma ray filter.

It should be noted that a further increase in the thickness of Bismuth filter, reduces the amount of gamma contamination

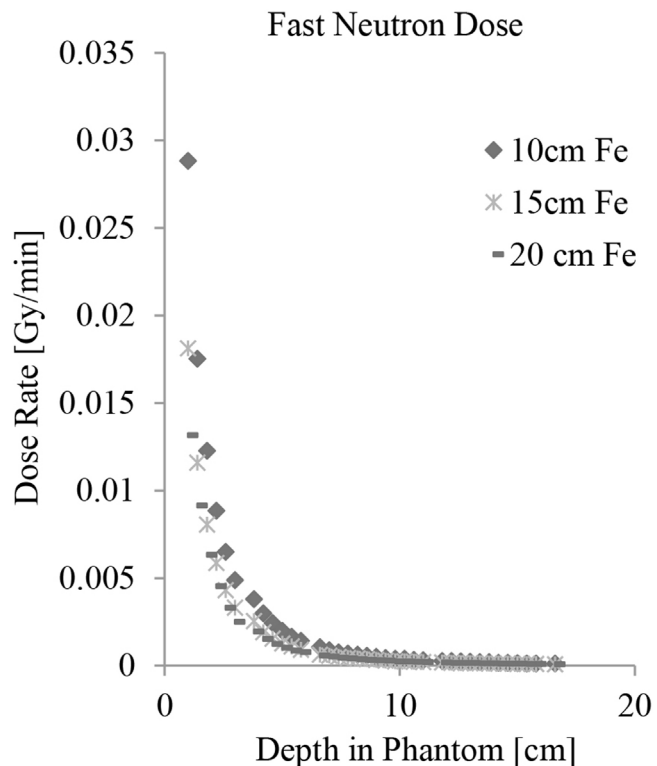


Fig. 4 – Comparison of the fast neutron dose, for different depths in the simulated head phantom for different thicknesses of iron moderator.

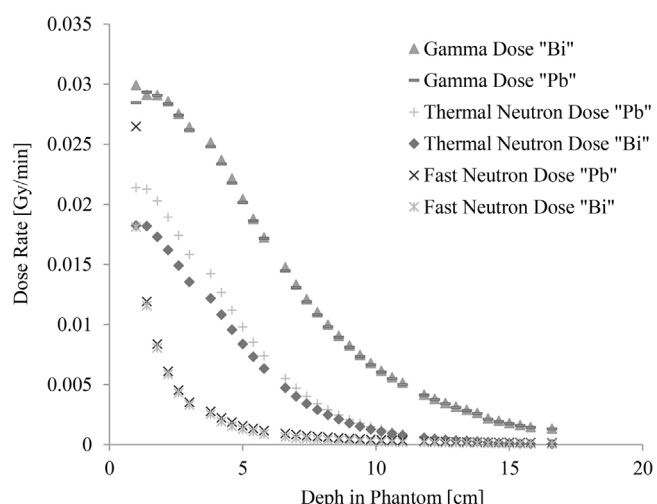


Fig. 5 – Comparison of the fast neutron dose, the thermal neutron dose and the gamma dose for different depths in the simulated head phantom for different gamma filters.

but decreases the epithermal neutron flux, which is obviously undesirable.

Compounds like Bi, B₄C and Li₂CO₃ can be used as a collimator to reflect neutrons back into the beam in order to achieve a better current-to-flux-ratio. Simulations for these three collimators for different diameters and thicknesses have been carried out and after obtaining their optimum values,

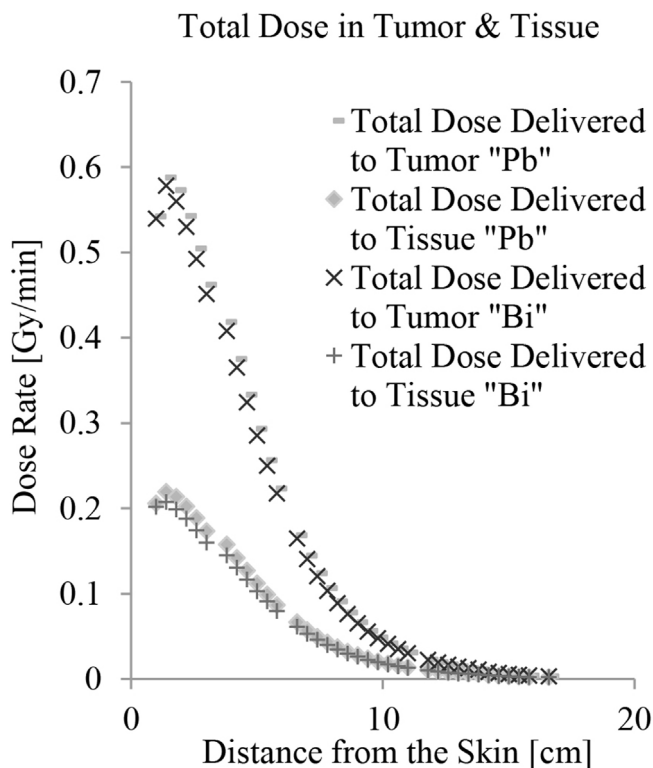


Fig. 6 – Comparison of the total delivered dose between tumor and normal tissues for different depths in the simulated head phantom for different gamma filters.

Table 7 – In-air measurements for different collimators.			
Neutron beam parameters	Bi	B ₄ C	Li ₂ CO ₃
$\emptyset_{\text{epi}}/\emptyset_{\text{fast}}$	2.73E1	3.13E1	2.16E1
$\emptyset_{\text{epi}}/\emptyset_{\text{th}}$	1.38E2	1.32E2	1.34E2
$\emptyset_{\text{epi}} [\text{n/cm}^2 \text{s}]$	3.94E6	3.94E6	1.71E6
$\bar{D}_{\text{fast}}/\emptyset_{\text{epi}} [\text{Gycm}^2/\text{n}]$	7.34E-15	2.25E-14	8.30E-15
$\bar{D}_{\gamma}/\emptyset_{\text{epi}} [\text{Gycm}^2/\text{n}]$	3.38E-14	6.14E-14	7.66E-14
$J_{\text{epi}}/\emptyset_{\text{epi}}$	0.797	0.814	0.898

in-air neutron beam parameters were summarized in Table 7. Although Li₂CO₃ has a much better performance than other collimators, it decreases the neutron flux. The reduction of epithermal neutron flux, if we use Li₂CO₃, is 43.5 percent compared to the Bi collimator.

On the other hand, although, B₄C has a better performance than Bi (Table 7), it increases the thermal and fast neutron dose (Fig. 7).

In addition to in-air neutron beam parameters, in-phantom measurements were calculated and they show that although thermal and gamma neutron doses are significantly reduced by Li₂CO₃ (Fig. 7), the dose which is delivered to tumor provided that we use this, is not as effective as Bi and B₄C (Fig. 8).

As a result, considering the above mentioned reasons, Bismuth was adopted as the best collimator.

Materials with high scattering cross section and high atomic mass (resulting in little energy loss), such as Lead or Bismuth, are used as a reflector.²⁶ As in this study reflec-

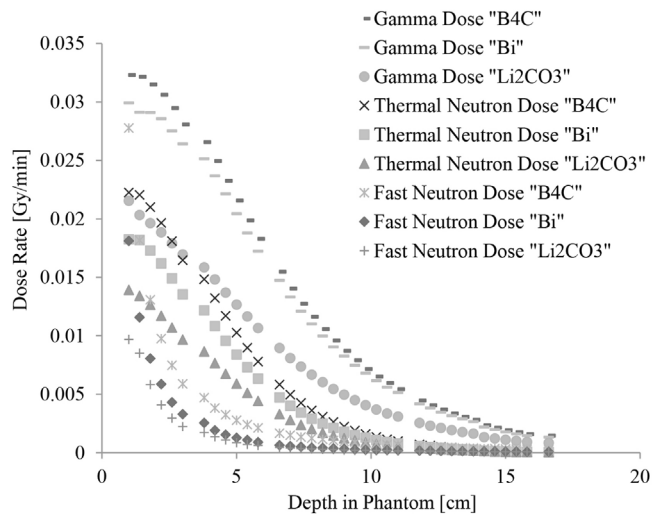


Fig. 7 – Comparison of the fast neutron dose, the thermal neutron dose and the gamma dose for different depths in the simulated head phantom for different collimators.

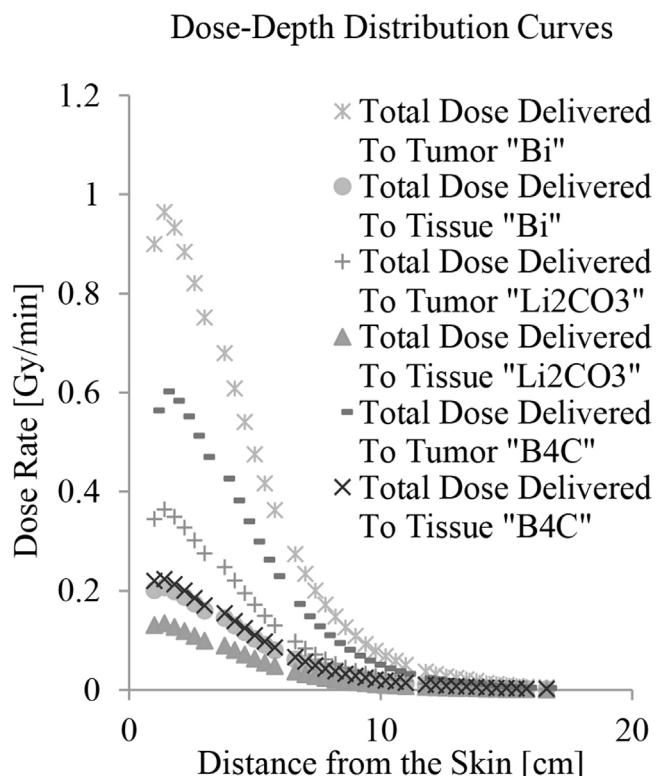


Fig. 8 – Comparison of the total delivered dose between tumor and normal tissues for different depths in the simulated head phantom for different collimators.

tor plays an additional role as a gamma shield, the following points should be considered:

- The fast neutron and gamma contamination around the BSA
- Designed neutron beam parameters

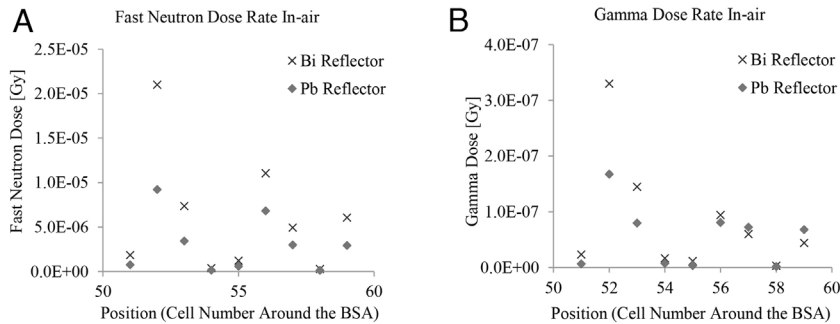


Fig. 9 – Comparison of fast neutron dose (A) and gamma dose (B) around the BSA for different reflectors.

Table 8 – Calculated free beam parameters for different reflectors.

Neutron beam parameters	Pb	Bi
$\emptyset_{\text{epi}}/\emptyset_{\text{fast}}$	2.73E+1	1.27E+1
$\emptyset_{\text{epi}}/\emptyset_{\text{th}}$	1.38E+2	3.09E+2
$\emptyset_{\text{epi}} [\text{n/cm}^2 \text{s}] (\text{Per Proton})$	6.07E-6	5.51E-6
$\dot{D}_{\text{fast}}/\emptyset_{\text{epi}} [\text{Gycm}^2/\text{n}]$	7.34E-15	1.95E-14
$\dot{D}_{\gamma}/\emptyset_{\text{epi}} [\text{Gycm}^2/\text{n}]$	3.38E-14	3.07E-14

To determine the amount of fast neutron and gamma contamination, some air spheres were placed around the BSA (Fig. 11) and determined (Fig. 9). In addition, designed neutron beam parameters are mentioned in Table 8. It can be seen that Lead not only reduces fast neutron dose, but also fast neutron and gamma contamination around the BSA. Therefore, Lead was used as both the reflector and the gamma shield.

4.2.1. Proposed configuration of BNCT irradiation facility
The final configuration of the BSA design is illustrated in Fig. 11. The proposed configuration has the following characteristics:

- Target – Tungsten - 7 cm diameter and 3 cm thickness
- Moderator - 15 cm of Iron + 105 cm of Aluminum + 21.3 cm Magnesium Fluoride (MgF_2)
- Thermal neutron absorber - 0.1 cm of Cadmium + 3 layer of Lithium Fluoride ($3 \times 0.1 \text{ cm}$)
- Reflector - Lead
- Collimator – 20 cm of Bismuth cone,
- Gamma shield – 0.5 cm of Bismuth,

4.3. Evaluation the proposed facility

With the BSA configuration and beam current of 104 nA, epithermal neutron flux of $3.94 \times 10^6 \text{ [n/cm}^2\text{]}$ can be achieved.

The purity of neutron beam, the dose rate of fast neutron to epithermal flux is $7.34 \times 10^{-15} \text{ [Gycm}^2/\text{n}]$ and the dose rate of gamma to epithermal flux is $3.38 \times 10^{-14} \text{ [Gycm}^2/\text{n}]$, which is comparable to most proposed or existing BNCT facilities. In addition, in Fig. 10, a very good spectrum shifting towards the epithermal energies can be observed: approximately, thermal flux presents 0.66%, epithermal flux 95.8% and fast flux 3.54% of the total neutron flux. The collimation of neutron beam is quite satisfactory: 0.797.

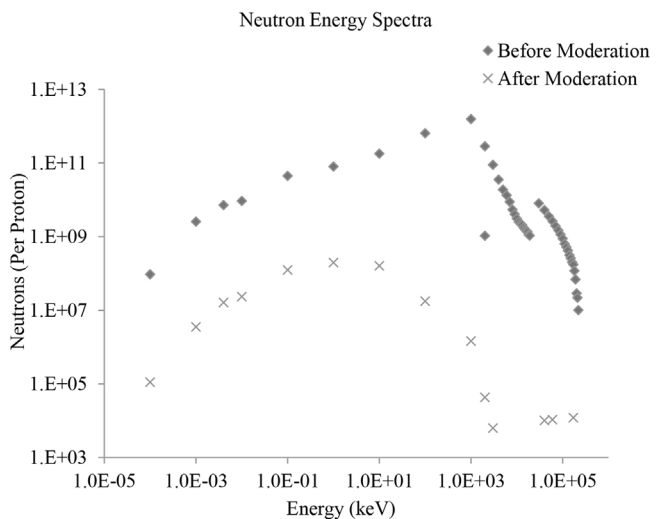


Fig. 10 – Neutron energy distribution before and after moderation corresponding to the optimal BSA.

This moderation satisfies IAEA recommended values in the beam exit window, except epithermal neutron flux. It would lead to the unacceptable treatment time of 55 h for a 104 nA proton beam current.

4.4. Proposed proton beam current

As mentioned in the previous section, the moderation would lead to the unacceptable treatment time of 55 h for a 104 nA proton beam. However, this unacceptably large treatment time could be reduced potentially by increasing the beam intensity, with a $5.75 \mu\text{A}$ proton beam current; this way the treatment time would shorten to 1 h. The therapeutic efficacy of neutron beam for the proposed BNCT facility and beam current of $5.75 \mu\text{A}$ was calculated through its in-phantom parameters as shown in Fig. 12.

With this moderation and for around 47 min irradiation time, the maximum dose of 38.2 Gy-eq can be delivered to tumor tissue at 1.4 cm from the phantom surface and the equivalent tumor dose of 24.1 Gy-eq can be achieved at the depth of 4.2 cm in the head phantom. This dose is limited by Brookhaven National Laboratory's (BNL) clinical trial protocol,²³ which suggests that the local equivalent dose to the

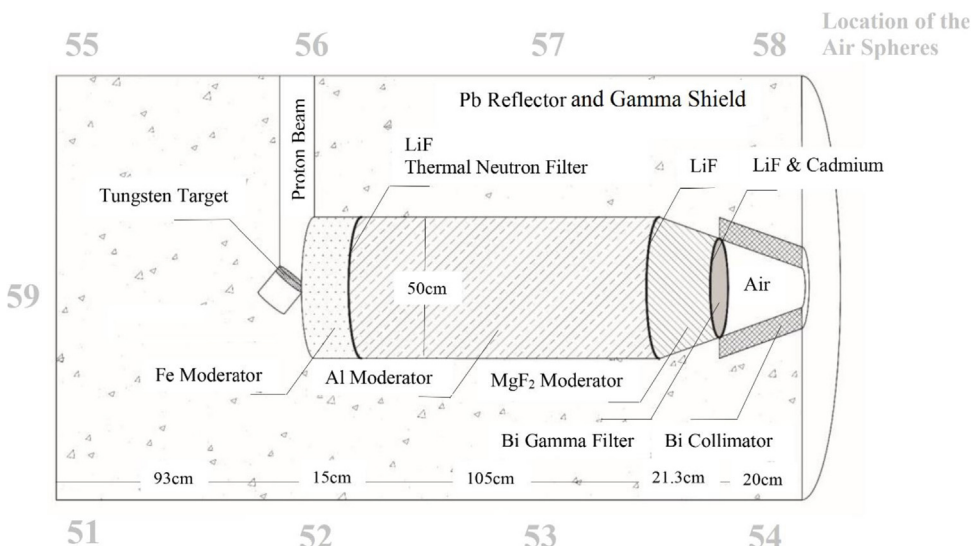


Fig. 11 – A cross-sectional view of the proposed BNCT facility modeling investigated in the present study.

Table 9 – In-phantom parameters evaluated for the proposed BSA and some other facilities.

Facility	ADDR (cGy/min)	TT (min)	AD (cm)	TD (cm)	Tumor: normal tissue ^{10}B concentration (ppm)
Proposed facility (provided that we use the beam current of 5.75 μA)	26.4	47:73	6.3	4	65:18
THOR ^a ²⁹	50	25	8.9	5.6	65:18
FiR 1 (Finland) ²⁹	45	30	9	5.8	65:18
R2-0 (Sweden) ²⁹	67	20	9.7	5.6	65:18
Kononov et al., 2004 ³⁰	100	12.5	9.1	–	65:18
FCB MIT ^b ³¹	125	10	9.3	–	65:18

ADDR, Advantage Depth Dose Rate; TT, Treatment Time; AD, Advantage Depth; TD, Therapeutic Depth.

^a Tsing Hua Open-Pool Reactor.

^b MIT Fission Converter Beam (FCB).

healthy tissue must not exceed 12.6 Gy. Thus, the treatment time will be limited by this value.^{27,28}

With intention to evaluate the proposed facility (provided that we use the beam current of 5.75 μA), the calculated

in-phantom parameters were compared with some BSA configurations of some previous published studies, which are listed in Table 9. In addition to in-phantom parameters, the calculated in-air neutron beam parameters of the proposed

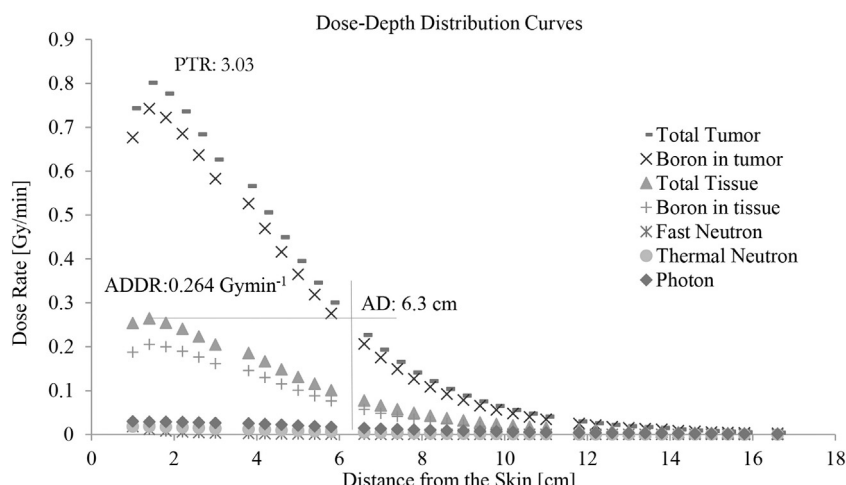


Fig. 12 – Depth dose rate profile along the beam axis as a function of depth in the head phantom (provided that we use the beam current of 5.75 μA).

Table 10 – In-air neutron beam parameters evaluated for the proposed BSA and eight BNCT facilities worldwide.³²

Facility	$\emptyset_{\text{thermal}}$ ($\times 10^8 \text{n/cm}^2 \text{s}$)	$\emptyset_{\text{epithermal}}$ ($\times 10^9 \text{n/cm}^2 \text{s}$)	\emptyset_{fast} ($\times 10^7 \text{n/cm}^2 \text{s}$)	$\dot{D}_{\text{fast}}/\emptyset_{\text{epithermal}}$ ($\times 10^{-13} \text{Gycm}^2/\text{n}$)
Proposed facility (provided that we use the beam current of 5.75 μA)	0.015	0.218	0.806	0.0734
FiR 1 (Finland)	0.66	1.03	3.2	1.4
BMRR ^a	0.14	0.68	3.0	2.6
Petten (Netherlands)	0.04	0.32	4.7	6.4
KURRI ^b	0.03	0.35	3.2	7.2
MIT-FCB	0.97	4.29	15.8	0.9
RA-6 (Argentina)	0.28	0.68	4.3	7.9
WSU (USA)	0.09	0.27	1.1	2.6
JAERI ^c	18	0.81	2.3	1.8

^a Brookhaven Medical Research Reactor.^b Kyoto University Research Reactor Institute.^c Japan Atomic Energy Research Institute.

facility and eight BNCT facilities worldwide are listed in Table 10.

5. Conclusions

In the present paper, the study is carried out using MCNPX2.6 code to evaluate the feasibility to use 230 MeV proton cyclotron in proton therapy centers as a spallation neutron source for BNCT. In this simulation, high-energy spallation neutrons produced by 230 MeV incident protons from Tungsten target were moderated by a configuration of Iron, Aluminum and Magnesium Fluoride as the best moderator materials. In addition, Lithium Fluoride and Cadmium as the thermal neutron filters and Bismuth as the gamma ray filter were used in the proposed BSA. Results for 230 MeV protons show that with the proposed BSA, proton beam current of about 5.75 μA is required to reduce the treatment time to an acceptable region of 47 min, which is accessible.

The biological dose evaluation in the simulated head phantom shows that if we use the beam current of 5.75 μA , the maximum dose of 38.2 Gy-eq can be delivered to tumor tissue at 1.4 cm from the phantom surface. In addition, it shows that the neutron beam produced this way has lower AD compared with other facilities. Hence, it is ineffective for the treatment of deep-seated tumors in the brain.

Conflict of interest

None declared

Financial disclosure

None declared

REFERENCES

- Barth RF, Soloway AH, Fairchild RG, Brugge RM. Boron neutron capture therapy: realities and prospects. *Cancer* 1992;70:2995–3001.
- Gong C, Tang X, Fatemi S, et al. A Monte Carlo study of SPECT in boron neutron capture therapy for a heterogeneous human phantom. *Int J Radiat Res* 2018;16(1).
- Yasui I, Kroc T, Gladden S, Andorf C, Bux S, Hosmane N. Boron neutron capture in prostate cancer cells. *Appl Radiat Isot* 2012;70(Jan (1)):6–12, <http://dx.doi.org/10.1016/j.apradiso.2011.07.001>.
- Trivillin VA, Serrano A, Garabalino MA, et al. Translational boron neutron capture therapy (BNCT) studies for the treatment of tumors in lung. *Int J Radiat Biol* 2019;95(May (5)):646–54, <http://dx.doi.org/10.1080/09553002.2019.1564080>.
- Locher GL. *Röntgenol. Am J. Radium Ther* 1936;36:1–13.
- Rasouli Fatemeh Sadat, S Farhad Masoudi. Simulation of the BNCT of Brain Tumors Using MCNP Code: Beam Designing and Dose Evaluation. *Iran J Med Phys* 2012, <http://dx.doi.org/10.22038/IJMP.2012.150>.
- Bavarnegin E, Kasesaz Y, Wagner F. Neutron beams implemented at nuclear research reactors for BNCT. *J Instrum* 2017, <http://dx.doi.org/10.1088/1748-0221/12/05/P05005>.
- Postuma I, Bortolussi S, Protti N, et al. An improved neutron autoradiography set-up for 10B concentration measurements in biological samples. *Reports of Practical Oncology & Radiotherapy*. 21. 10.1016/j.rpor.2015.10.006.
- World-Wide Neutron and Proton Facilities, North American Facilities, JESD89 update/version July (2005).
- MCNPX User's Manual Version 2.6.0, LA-CP-02-408. Los Alamos National Laboratory; 2008.
- Fantidis JG. *J Theor Appl Phys* 2018;12:249, <http://dx.doi.org/10.1007/s40094-018-0312-1>.
- Filges D, Goldenbaum F. Handbook of spallation research: theory, experiments and applications. Wiley; 2010, <http://dx.doi.org/10.1002/9783527628865.ch10>. ISBN: 978-3-527-40714-9.
- Carpenter JM. *Nucl Instr Methods* 1977;145:91–113.
- White Marion, Project, SNS. Spallation neutron source (SNS); 2002, <http://dx.doi.org/10.1063/1.1472000>.
- Review of the neutron science laboratory KENS in the high energy accelerator research organization KEK. Japan: Technical Report; 2004.
- Los alamos neutron science center; 2012 <http://lansce.lanl.gov/>.
- Rutherford appleton laboratory; 2012 <http://www.isis.stfc.ac.uk/>.
- Swiss spallation neutron source; 2012 <http://www.psi.ch/sinq/>.
- Gardner I. A review of spallation neutron source accelerators; 2019.
- International Atomic Energy Agency (IAEA), Current status of neutron capture therapy, in IAEA-Tecdoc-1223. 2001, IAEA: Wien.

21. Soppera N, Dupont E, Bossant M. JANIS Book of neutron-induced cross-sections; 2012.
22. Rahmani F, Shahriari M. Dose calculation and in-phantom measurement in BNCT using response matrix method. *Appl Radiat Isot* 2011;69(Dec (12)):1874–7, <http://dx.doi.org/10.1016/j.apradiso.2011.02.019>.
23. Chanana AD. Boron Neutron Capture Therapy of Glioblastoma Multiforme at the Brookhaven Medical Research Reactor, A Phase I/II Study, FDA IND 43317, Protocol 4. Upton, NY: Medical Department, Brookhaven National Laboratory; 1996. p. 11973.
24. Snyder WS, Ford MR, Warner GG, Fisher Jr HL, country unknown/code not available: n. p. Estimates of absorbed fractions for monoenergetic photon sources uniformly distributed in various organs of a heterogeneous phantom; 1969.
25. Ghal-Eh N, Goudarzi H, Rahmani F. FLUKA simulation studies on in-phantom dosimetric parameters of a LINAC-based BNCT. *Radiation Physics and Chemistry* 141. 36–40. <https://doi.org/10.1016/j.radphyschem.2017.06.004>.
26. Knoll GF. *Radiation detection and measurements*. New York: Wiley; 1979.
27. Kasesaz Y, Rahmani F, Bavarnegi E. Evaluation of boron neutron capture therapy in-phantom parameters by response matrix method. *J Cancer Res Ther* 2018;14:1065–70, <http://dx.doi.org/10.4103/0973-1482.187288>.
28. Rasouli FS, Masoudi SF, Kasesaz Y. Design of a model for BSA to meet free beam parameters for BNCT based on multiplier system for D-T neutron source. *Ann Nucl Energy* 2012;39:18–25. January. <https://doi.org/10.22038/IJMP.2012.150>.
29. Liu YW, Huang TT, Jiang SH, Liu HM. Renovation of epithermal neutron beam for BNCT at THOR. *App Radiat Isot* 2004;61(5):1039–43, <http://dx.doi.org/10.1016/j.apradiso.2004.05.042>.
30. Kononov OE, Kononov VN, Bokhovko MV, et al. Optimization of an accelerator-based epithermal neutron source for neutron capture therapy. *Appl Radiat Isot* 2004;61:1009–13, <http://dx.doi.org/10.1016/j.apradiso.2004.05.028>.
31. Birns PJ, Riley KJ, Ostrovsky Y, et al. Improved dose targeting for a clinical epithermal neutron capture beam using optimal ^{6}Li filtration. *Int J Radiat Oncol Biol Phys* 2007;67(5):1484–91.
32. Auterinen IH, Serén T, Anttila K, Kosunen A, Savolainen S. Measurement of free beam neutron spectra at eight BNCT facilities worldwide. *Appl Radiat Isot* 2004, <http://dx.doi.org/10.1016/j.apradiso.2004.05.035>.